Biochemistry (Moscow), Vol. 68, No. 4, 2003, pp. 436-445. Translated from Biokhimiya, Vol. 68, No. 4, 2003, pp. 537-547.

Change in pH-dependent Membrane Insertion Characteristics of Trichosanthin Caused by Deletion of Its Last Seven C-terminal Amino Acid Residues

Fan Zhang[1], Ying-Jie Lu[1], Pang Chui Shaw[2], and Sen-fang Sui[1]*

[1]Department of Biological Sciences and Biotechnology, State Key Laboratory of Biomembranes, Tsinghua University, Beijing 100084, P. R. China; fax: (86)-10-62784768; E-mail: suisf@mail.tsinghua.edu.cn
[2]Department of Biochemistry, Chinese University of Hong Kong, Hong Kong, China

Received March 7, 2002
Revision received June 27, 2002

Abstract—Trichosanthin (TCS) is a type I ribosome-inactivating protein (RIP) that can selectively kill some types of cells at low concentration (0.1-1 nM). The pH-dependent membrane insertion ability of TCS makes it possible that the internalized toxin avoids degradation in lysosomes and further undergoes transportation into the cytosol by some still unidentified mechanism. Here, we show that deletion of C-terminal residues affects interactions of modified TCS (C7-TCS) with lipids and reduces its pH-dependent membrane insertion ability. Fluorescence measurements indicate that at low pH C7-TCS undergoes profound conformational changes that causes exposure of a hydrophobic region and leads to oligomerization of the C7-TCS molecules. The results suggest that the membrane insertion of TCS at low pH might be important for translocation of TCS into the cytosol, which is important for exertion of the RIP activity of TCS. Deletion of the last seven C-terminal residues of TCS would reduce both its RIP activity *in vitro* and cytotoxicity *in vivo*, with the degree of decrease being more significant for the cytotoxicity *in vivo*.

Key words: conformation change, lipid–protein interaction, membrane surface pressure, ribosome-inactivating protein, trichosanthin

Trichosanthin (TCS) is a toxin isolated from the root tuber of *Trichosanthes kirilowi maxim* [1, 2]. It belongs to the type I ribosome-inactivating proteins (RIP), and consists of a single polypeptide chain. TCS can remove adenine 4324 of 28S rRNA, owing to its N-glycosidase activity [3, 4], thus preventing binding of EF-2 and GTP by ribosome and causing arrest of protein synthesis [5]. TCS is capable of killing some types of cells, such as syncytiotrophoblast cells, JAR cells, K562 cells, etc. [6-8] at low concentrations (0.1-1 nM).

As ribosomes, the target substrates of RIPs, are located in the cytosol of mammalian cells, the translocation of an internalized toxin into the cytosol is necessary to exert its RIP function. The mechanism of type II RIP translocation has only recently been clarified to some extent [9]. The type II RIP consists of two polypeptide chains: the A-chain has enzymatic activity and the B-chain is a lectin-like protein. Two pathways have been identified for the type II RIPs. First, at low pH in the endosome, the B-chain of internalized toxin penetrates into the membrane and forms a cation-selective channel; then the A-chain travels through the channel into the cytosol, similarly to diphtheria toxin [9-14]. Second, after endocytosis, the holotoxin is transported from the endosome to the ER through the Golgi apparatus. Then the A-chain enters the cytosol by a mechanism involving the Sec61 complex, in the same way as ricin and shiga toxins do [15-23]. For all the type II RIPs, the lectin activity of the B-chain is necessary for transmembrane translocation. In fact the cytotoxicity is lost in the case of free A-chain or the holotoxin with mutant B-chain. However, they still could be internalized into cells by fluid phase endocytosis instead of receptor mediated endocytosis [23, 24]. Recent investigation indicated that the ricin B-chain can promote the translocation of holo-

Abbreviations: TCS) trichosanthin; C4-TCS) modified trichosanthin lacking four C-terminal amino acid residues; C7-TCS) modified trichosanthin lacking seven C-terminal amino acid residues; RIP) ribosome-inactivating protein; ER) endoplasmic reticulum; DMPS) 1,2-dimyristoyl-*sn*-glycerol-3-phosphatidylserine; DPPC) 1,2-dipalmitoyl-*sn*-glycerol-3-phosphatidylcholine; DPPG) 1,2-dipalmitoyl-*sn*-glycerol-3-phosphatidylglycerol.

* To whom correspondence should be addressed.

0006-2979/03/6804-0436$25.00 ©2003 MAIK "Nauka/Interperiodica"

toxin from Golgi to ER by interaction with some Golgi/ER glycoproteins.

The type I RIPs consist of a single polypeptide chain which has similar amino acid sequence and structure with the A-chain of the type II RIPs. The type I RIPs are unable to bind to receptors with carbohydrate groups due to the lack of lectin fraction. They enter the cell only by nonspecific fluid phase endocytosis [25]. Strong cytotoxicity of the type I RIPs (such as TCS, saporin-S6, etc.) on their sensitive cells suggests that the internalized toxin is able to inactive ribosomes by entering the cytosol from membrane limited organelles (such as endosome, lysosome, or endoplasmic reticulum (ER)). However, the translocation mechanism of the type I RIPs not involving B-chain is still unclear. Some other unidentified factors may take part in the complex process. In previous works [26-28], the membrane insertion ability of TCS was found to be pH-dependent, with the membrane insertion of TCS being induced at low pH (e.g., pH 4.6). This finding suggests that membrane insertion of internalized TCS at low pH causes a number of TCS molecules to avoid degradation in lysosomes, and then they might further be translocated into the cytosol by mediation of a channel on the endosome membrane (similar with diphtheria toxin), or by involvement of Sec61 complex on the ER membrane (similar with ricin toxin), or in a still unclear manner. Based on this point of view, change in pH-dependent membrane insertion ability of TCS will change the number of translocated TCS molecules, thus affect its cytotoxicity.

C7-TCS, a mini-TCS, was prepared by deleting the last seven amino acid residues in the flexible C-terminal tail of TCS. The *in vivo* assay indicates that cytotoxicity of C7-TCS is 12 times less than that of TCS, though it is still a potent cytotoxin (IC_{50} = 2.01 nM) [29]. To reveal whether the decrease in cytotoxicity of C7-TCS was affected by the change in pH-dependent membrane insertion ability, in the present work the interaction of C7-TCS with lipid membrane was investigated. The results showed that the deletion of the C-terminal amino acid residues resulted in reduced pH-dependent membrane insertion ability of TCS. Moreover, fluorescence measurements showed that the deletion also induces instability of the tertiary structure of C7-TCS and results in the oligomerization of C7-TCS. These results suggest that deleting the last seven amino acid residues of the TCS C-terminal might affect its translocation into the cytosol and cause a decrease in its cytotoxicity.

MATERIALS AND METHODS

Materials. The following chemicals were purchased from Sigma (USA): 1,2-dimyristoyl-*sn*-glycerol-3-phosphatidylserine (DMPS), 1,2-dipalmitoyl-*sn*-glycerol-3-phosphatidylcholine (DPPC), 1,2-dipalmitoyl-*sn*-glycerol-3-phosphatidylglycerol (DPPG). Other chemicals (analytical grade) were made in China.

Preparation of trichosanthin mutants. Vector for expression of C4-TCS and C7-TCS in *E. coli* were constructed as described in Chan et al. [29]. PCR mutagenesis of trichosanthin using high fidelity *Pfu* DNA polymerase was carried out with pET58210 using the oligonucleotide sequence encoding wild-type trichosanthin [30]. The PCR products were cleaved by *Nco*I and *Bam*HI and cloned in pET8c [31] for over expression. The PCR amplified DNA was sequenced by a T7 sequencing kit (Amersham Pharmacia Biotech, Sweden) to avoid secondary mutation. Protein expression and purification were performed as described in Wong et al. [32]. The deleted amino acid sequences (C4 and C7) are shown in Table 1.

Monolayer study. Monolayer surface pressure was measured using the Wilhelmy plate method [33] with a NIMA 9000 microbalance (Nima Technology Ltd, U.K.). Surface pressure (π) was defined as the surface tension difference before and after depositing the monolayer on the solution surface. All the data were collected automatically and recorded by a personal computer. The homemade sample trough [34, 35] had a volume of 4 ml and a surface area of 10 cm^2. The sub-phase was stirred continuously with a magnetic bar. In the experiment, the phospholipid was dissolved in chloroform–methanol mixture (3 : 1 v/v) at a concentration of 1.0 mg/ml and coated onto the buffer surface to form a lipid monolayer. After stabilization of the surface pressure at a designated value, which was considered as initial surface pressure (π_i), the solution of C4-TCS and C7-TCS at appropriate concentrations was injected into the sub-phase through a side sample hole. The pressure change was monitored until the surface pressure increase ($\Delta\pi$) had reached a maximum value (usually within 2 h). All the experiments were carried out under N_2 to prevent oxidation of the samples. The temperature of the system was maintained at 25 ± 0.2°C.

Table 1. C-Terminal amino acid sequence of wild-type and mutant forms of TCS

Protein	C-Terminal amino acid sequence
TCS	Ile^{237}-Ala-Leu-Leu-Leu-Asn-Arg-Asn-Asn-Met-(Ala^{247})*
C4-TCS	Ile^{237}-Ala-Leu-Leu-Leu-Asn-Arg-$\underline{Asn^{244}}$-Asn-Met-($\underline{Ala^{247}}$)**
C7-TCS	Ile^{237}-Ala-Leu-Leu-$\underline{Leu^{241}}$-Asn-Arg-Asn-Asn-Met-($\underline{Ala^{247}}$)**

* C-Terminal amino acid sequence of wild-type TCS includes two isoforms: -Asn-Asn-Met-Ala-OH and -Asn-Asn-Met-OH.

** Underlined amino acid sequence indicates the deleted amino acids in trichosanthin mutants.

As reported earlier, the surface pressure increases when a protein becomes embedded into the monolayer, but does not increase if the protein interacts only with the phospholipid head groups [36]. Thus, when protein molecules are injected into the sub-phase, corresponding change in the surface pressure ($\Delta\pi$) can be interpreted as the result of protein insertion into the lipid monolayer. $\Delta\pi$ can be obtained at various π_i for each sample. The plot of $\Delta\pi$ versus π_i then yields a straight line with negative slope intersecting the abscissa at a limiting surface pressure. The limiting surface pressure, defined as critical insertion pressure (π_c) of the protein sample for corresponding lipid monolayer, was used for quantitative evaluation of the insertion ability of the protein in the phospholipid monolayer.

Fluorescence measurements. Fluorescence wavelength scanning was performed with Hitachi F-2500 fluorescence spectrophotometer (Japan) using a 1-cm^2 quartz fluorescence cuvette, and the results were processed by its fluorescence data management software. The C7-TCS solution, and Trp solution for control, were diluted to 2 μM with citrate-phosphate buffer of indicated pH and then quickly mixed to homogeneous state. Ten minutes later fluorescence measurement was performed. The excitation wavelength was 280 nm, and the emission was scanned in the interval of 295-400 nm. The emission and excitation slits were 5 and 10 nm, respectively. The background spectra of the buffer were subtracted. The scanning speed was 60 nm/min. The experiments were carried out at 25 ± 0.2°C.

The fluorescence polarization (FP) technique was first described in 1926 [37], and in recent years has been widely used to reveal molecular interactions [38-42]. This approach is based on the observation that if one excites a fluorophore with plane-polarized light, the emitted light will be polarized as well. The angle between the planes of exciting and emitted light is highly dependent on the molecular motion of the fluorophore. The degree of steady-state polarization, *P*, is defined from the following equations:

$$P = (I_{VV} - G \times I_{VH})/ (I_{VV} + G \times I_{VH});$$

$$G = I_{HV} / I_{HH};$$

$$V = 0\,^\circ; H = 90\,^\circ,$$

where I_{VV} and I_{VH} are the intensities of vertically and horizontally polarized emission with vertically polarized incident light; *G*, the grating factor defined as I_{HV}/I_{HH} with horizontally polarized incident light, is a wavelength-dependent polarization response of components of an emission system. If the fluorophore-containing molecules are aggregated, the rotational relaxation time increases because of slower rotation of the molecular aggregates [37], which results in increased *P* value.

The FP measurements were performed with a Hitachi F-4010 fluorescence spectrophotometer using a 1-cm^2 quartz fluorescence cuvette. For each sample, the I_{VV}, I_{VH}, I_{HH}, and I_{HV} were measured three times. The excitation wavelength was at 280 nm and the emission wavelength corresponded to the emission maximum (λ_{max}) of C7-TCS at the indicated pH. The emission and excitation slits were 5 and 10 nm. Scanning speed was 120 nm/min. The fluorescence background of the buffer was subtracted. Experiments were carried out at 25 ± 0.2°C.

CD spectrometry. CD measurements were carried out with a Jasco J-715 spectropolarimeter. Samples containing C7-TCS at a concentration of 3 μM were scanned at least four times at the rate of 100 nm/min and averaged. The temperature of the sample compartment was maintained at 25 ± 0.2°C with a water-circulating bath. The path length of the quartz cell was 2 mm. For correction, a blank run made with the appropriate pH buffer alone was subtracted from the spectra. The spectra at 200-250 nm were used for analysis and calculation. All the spectra were smoothed and converted into molar ellipticity using an average residue molecular mass of 110 daltons.

RESULTS

Monolayer measurements. *Membrane insertion ability of C4- and C7-TCS into different phospholipid monolayers.* In the beginning, the penetration of C4- and C7-TCS into the air/water interface without phospholipid monolayer was measured. In the experiments, the sub-phase concentrations of C4- and C7-TCS were 50, 100, 150, and 200 nM. The results showed that the maximum $\Delta\pi$ values induced by C4- and C7-TCS were 14 and 11 mN/m, respectively. Therefore, in the following protein insertion experiments the π_i values of phospholipid monolayers were kept at or above 15 mN/m. The interactions of C4- and C7-TCS with monolayers of DPPG, DMPS, and DPPC were studied with their 200 nM solution. In the measurements, pH 4.6 was chosen, which corresponds to optimal pH for membrane insertion of TCS [27]. Figure 1 shows the $\Delta\pi$ versus π curves for C4- and C7-TCS interacting with different phospholipid monolayers. The values of π_c characterizing interaction of C4-TCS with DPPG and DMPS are 31 and 29 mN/m, respectively; those for C7-TCS with DPPG, DMPS, and DPPC are 27.4, 28.0, and 26.9 mN/m, respectively (Table 2).

In comparison with TCS, these results indicate that C4- and C7-TCS clearly exhibit distinctions in their membrane insertion characteristics at least as to the following points. First, although to different degree, membrane insertion ability of C4- and C7-TCS into negatively charged phospholipid monolayers is decreased, with

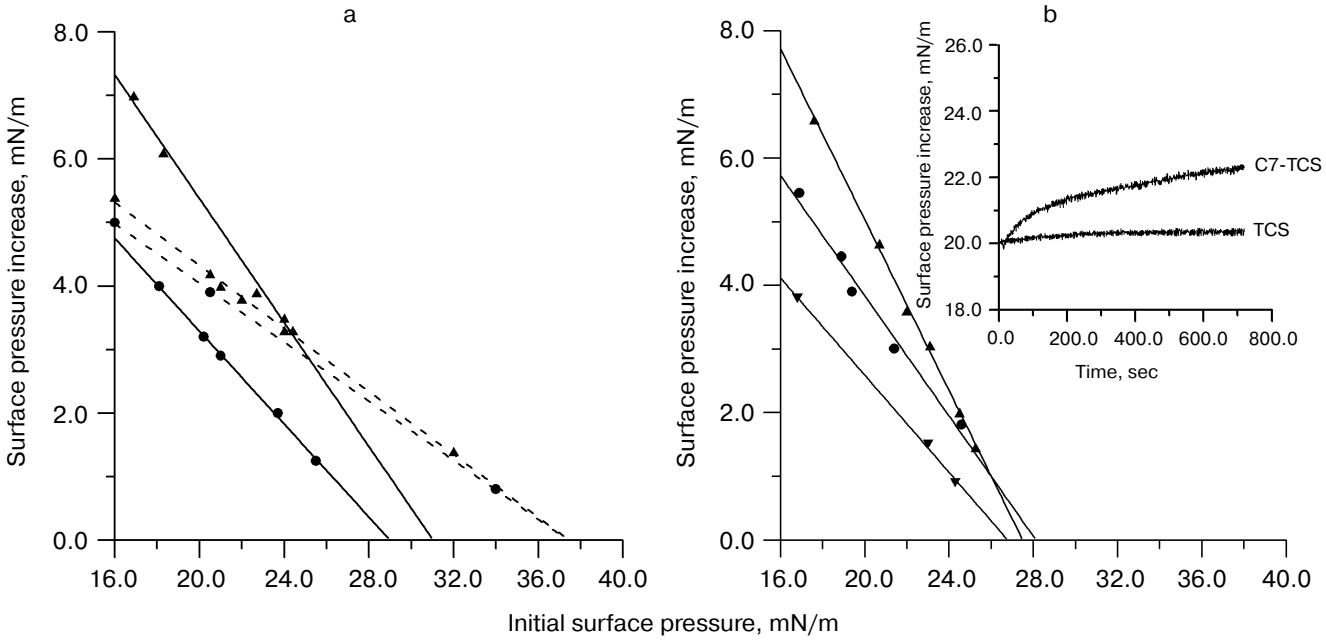

Fig. 1. Membrane insertion $\Delta\pi$ versus π curves for trichosanthin mutants on different phospholipid membranes. The final concentration (saturation) of C4- and C7-TCS in the sub-phase was 200 nM. The sub-phase buffer was citrate-phosphate, pH 4.6. The experiments were carried out at 25 ± 0.2°C. a) Membrane insertion $\Delta\pi$ versus π curve for C4-TCS (solid line) and TCS (dashed line) on DMPS (●) or DPPG (▲) monolayer. b) Membrane insertion $\Delta\pi$ versus π curve for C7-TCS on DMPS (●), DPPG (▲), or DPPC (▼) monolayer. The inset graph is the membrane insertion π versus *t* curve of TCS and C7-TCS on DPPC monolayer; initial surface pressure was 20 mN/m.

C4-TCS occupying an intermediate position between TCS and C7-TCS. Second, C7-TCS interacts similarly with both negatively charged and neutral phospholipids at pH 4.6. As Fig. 1b and Table 2 show, C7-TCS is characterized by similar π_c values for both negatively charged (DPPG and DMPS) and neutral (DPPC) phospholipids. In contrast to TCS, the difference in membrane insertion ability of C7-TCS into charged and non-charged monolayer is minimal. Previous work [25] has shown that TCS does not interact with DPPC monolayer at pH 4.6, even at lower initial monolayer pressure. Here the addition of C7-TCS led to obvious increase in the surface pressure on the DPPC monolayer (as shown in the inset graph of Fig. 1b).

Effect of pH on membrane insertion of C7-TCS. Figure 2 shows the results of further experiments on the pH dependence of membrane insertion of C7-TCS. The plots in Fig. 2a show that $\Delta\pi$ increases with decreasing sub-phase pH at the same π_i. Such behavior is similar to that of TCS. However, certain disparity between C7-TCS and TCS in the pH dependence can be found. In the case of TCS, $\Delta\pi$ increased with decreasing sub-phase pH in the pH region 5.8-4.6 and reached maximum $\Delta\pi$ at pH 4.6 [27]. Above and below this pH region $\Delta\pi$ was not sensitive to pH variations [27]. However, in case of C7-TCS, the $\Delta\pi$ versus pH curve did not show a maximum at pH about 4.6, and $\Delta\pi$ continued to increase until pH 2.94 (Fig. 2a). The plots of Fig. 2b show π_c value for C7-TCS at two different pH values, i.e., 27.4 mN/m at pH 4.6 and 35 mN/m at pH 2.94. Even at pH 2.94 the π_c value for C7-TCS is still obviously lower than that of TCS at pH 4.6 (about 38 mN/m). These results suggest that deletion of C-ter-

Table 2. Critical insertion pressure of wild-type and mutant TCS on different phospholipid monolayers

Protein	Phospholipid		
	DPPG, mN/m	DMPS, mN/m	DPPC, mN/m
TCS*	37.5	37.5	—**
C4-TCS	31	29	n.d.***
C7-TCS	27.4	28	26.9

Note: Final concentrations (saturating concentrations) of C4- and C7-TCS in the sub-phase were 100 and 200 nM, respectively. Citrate-phosphate buffer, pH 4.6, was used as the sub-phase solution.
* These data were obtained from [28].
** There is no interaction between wild-type TCS and DPPC.
*** n.d., not determined.

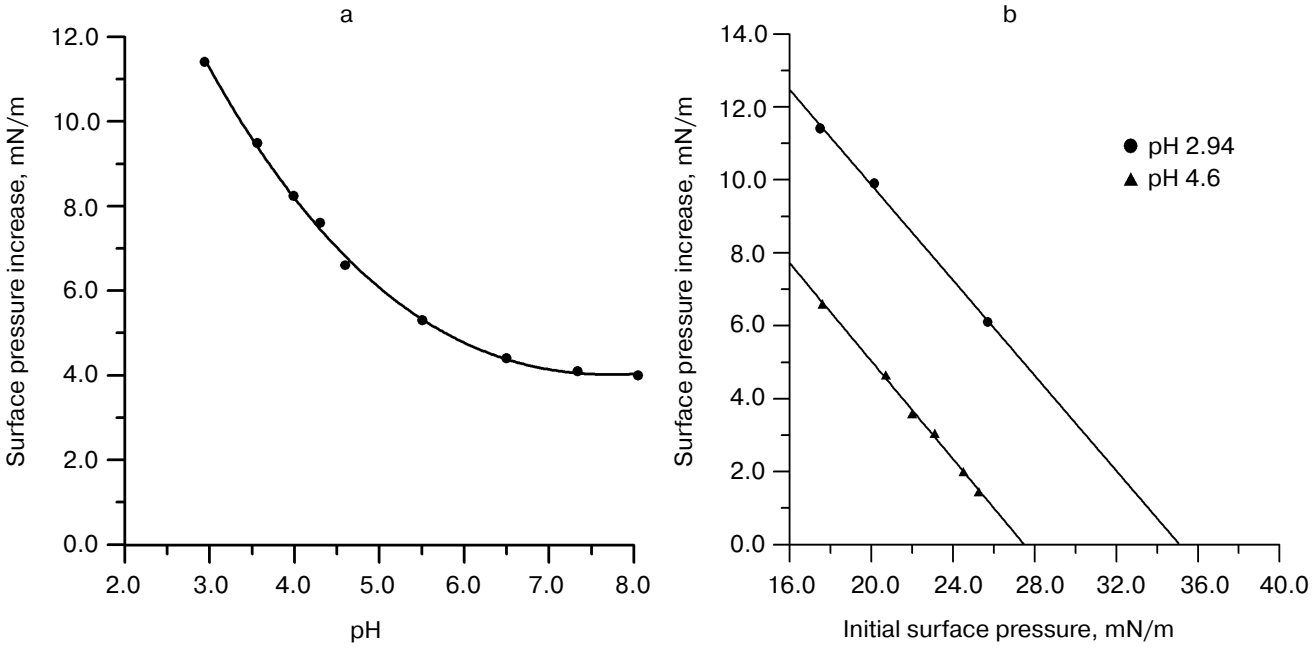

Fig. 2. Influence of pH on insertion of C7-TCS into DPPG monolayer. Initial monolayer pressure was kept at 17.6 ± 0.2 mN/m. Final concentration of C7-TCS in the sub-phase was 200 nM. Citrate-phosphate buffer was used for all pH values. All experiments were carried out at 25 ± 0.2°C. a) Membrane insertion Δπ versus pH curve for C7-TCS on DPPG monolayer. b) Membrane insertion Δπ versus π curves for C7-TCS on DPPG monolayer at sub-phase pH 2.94 and 4.6.

minal residues of TCS significantly alters its pH-dependence of membrane insertion.

Effect of ionic strength on membrane insertion of C7-TCS. Electrostatic force plays an essential role in the interaction of TCS with negative charged phospholipids, as reported earlier by Xia et al. [25] and Lu et al. [37]. Since TCS is an alkaline protein (pI = 9.4), it carries more positive charges at lower pH (e.g., at pH 4.6). This facilitates the docking of TCS on negatively charged lipid and its insertion into the membrane through conformational changes. The electrostatic interactions can be inhibited by high ion strength (e.g., in the presence of 300 mM NaCl). Thus, the membrane insertion of TCS into DPPG was significantly reduced with increasing Na^+ concentration and rendered almost undetectable when [Na^+] approached 300 mM. On the other hand, for C7-TCS addition of NaCl solution into pH 4.6 buffer exhibited no visible effect on its membrane insertion ability into DPPG monolayer (Fig. 3). The increased surface pressure induced by injection of C7-TCS at 400 mM Na^+ concentration is nearly identical to that in the presence of 100 mM Na^+ concentration. This phenomenon suggests that, unlike TCS, interaction of C7-TCS with the membrane is not sensitive to ionic strength.

Fluorescence measurements. Membrane insertion of soluble proteins is frequently accompanied by conformational changes, since almost all of their surface amino acids are charged or hydrophilic. Such conformational changes presumably cause exposure of hydrophobic regions, which enables insertion into hydrophobic core of a lipid membrane.

TCS has a single Trp residue located in the turn in the H7 region. Fluorescence intensity and λ_{max} of Trp intrinsic fluorescence is influenced by its interaction with other molecular structures and microenvironment, in particular a hydrophobic one. Therefore, the conformational changes in TCS and C7-TCS can be tested by measuring changes in their Trp fluorescence characteristics.

The experiments were performed at various pH values (7.2, 4.5, 4.1, 3.64, and 2.98). At pH 7.2, the λ_{max} of C7-TCS for 280 nm excitation was 337 nm, with a red shift of approximately 10 nm, compared with 327.5 nm for wild TCS. This result is identical with that previously reported [28], where the red shift was interpreted as being due to a relaxing effect of helix H7. Along with decreasing pH, the intrinsic fluorescence intensity of C7-TCS was distinctly reduced until the pH reached 3.64, and in the meanwhile the λ_{max} of Trp fluorescence showed a gradual blue shift to 332 nm (Fig. 4a and Table 3). As a control, variation of pH had just a minor effect on the fluorescent characteristics of free Trp and wild TCS (Fig. 4, a and b). There was no shift in λ_{max}, and only an insignificant change in the fluorescence intensity was observed for both free Trp and wild TCS.

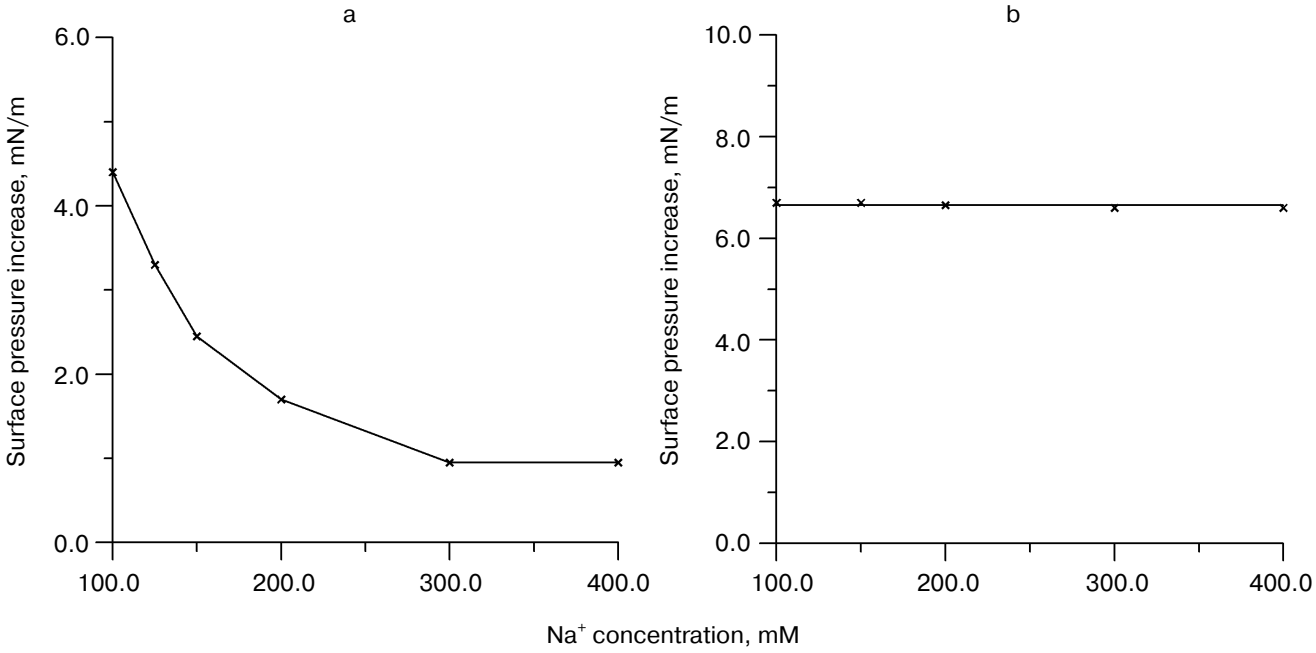

Fig. 3. Effect of sub-phase ionic strength on membrane insertion of C7-TCS. a) Effect of Na^+ concentration on membrane insertion of TCS (from [36]). b) Effect of Na^+ concentration on membrane insertion of C7-TCS into DPPG monolayer. The initial monolayer pressure was 17.6 ± 0.2 mN/m. The sub-phase solution was citrate-phosphate buffer containing appropriate concentration of Na^+, pH 4.6. The experiments were carried out at 25 ± 0.2°C.

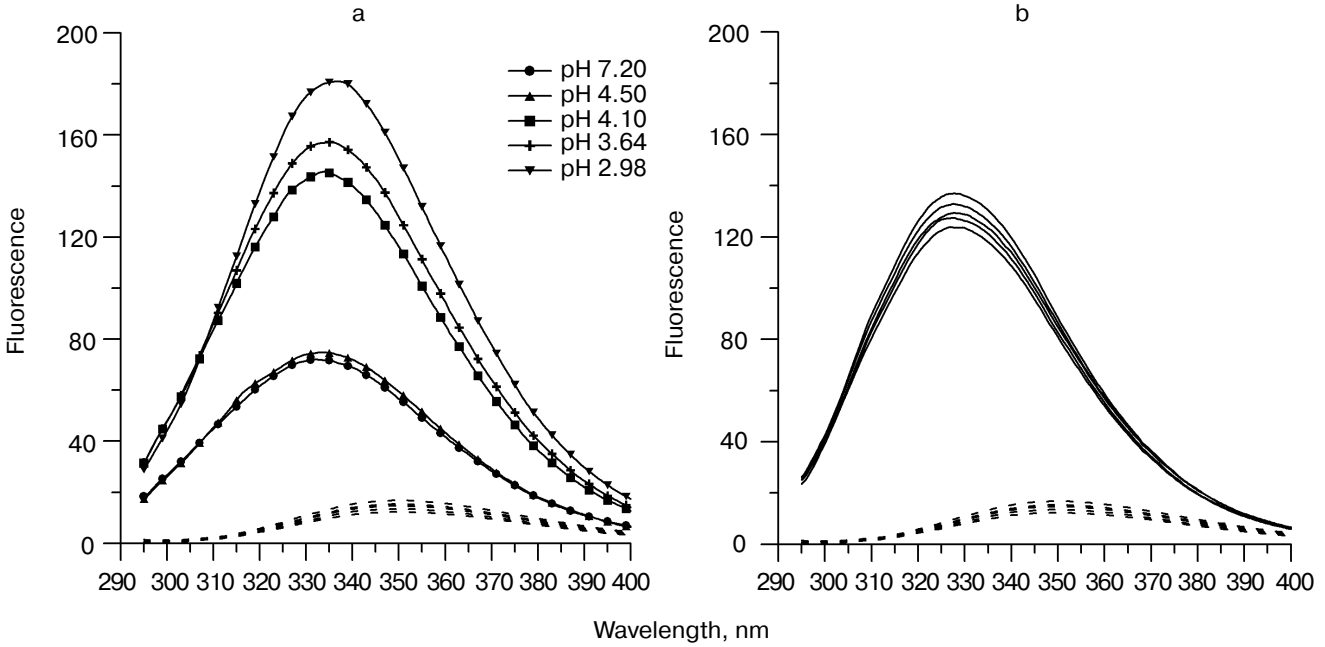

Fig. 4. Effect of pH on Trp fluorescence of C7-TCS and wild-type TCS. Before experiments, the samples were diluted with citrate-phosphate buffer at indicated pH to 2 μM for C7-TCS and free Trp, and to 1.5 μM for wild-type TCS. Ten minutes later, the 295-400 nm spectrum was scanned with excitation at 280 nm. The pH values were decreased to 7.2, 4.5, 4.1, 3.64, and 2.98, respectively, from the bottom to the top. The experiments were carried out at 25 ± 0.2°C. a) Trp fluorescence of C7-TCS (solid line) and of free Trp (dashed line) at different pH values. b) Trp fluorescence of TCS (solid line) and of free Trp (dashed line) at different pH values.

Fluorescence polarization is a useful tool for detecting a change in aggregation state of a protein in solution. If protein molecules undergo aggregation, the value of fluorescence polarization will increase owing to slower rotation of the molecular aggregates. The fluorescence polarization measurements were carried out at various pH values—7.2, 4.5, and 4.1. The fluorescence intensity of C7-TCS at pH 3.64 and 2.98 was too low to be detected. Figure 5 and Table 4 show that the *P* value of C7-TCS increases with decreasing pH. In addition, the change in fluorescence polarization was found to be a rather rapid process, with the effect manifesting itself a few minutes after injection of C7-TCS into the indicated pH buffer and remaining stable for several hours.

CD measurements. The changes in fluorescence characteristics of C7-TCS signify that decrease in pH value induces conformational rearrangement of C7-TCS. If this concerns the elements of secondary structure, there must be detectable changes in the CD spectrum. With this in mind, CD spectra (200-250 nm) of C7-TCS in different pH buffers were examined. The results are given in Table 4, in which the contents of α-helices, β-sheets, β-turns, and random coils were estimated using the method of Yang et al. [43]. Table 4 shows that, similarly with TCS, secondary structure of C7-TCS remained relatively invariant at various pH values [25].

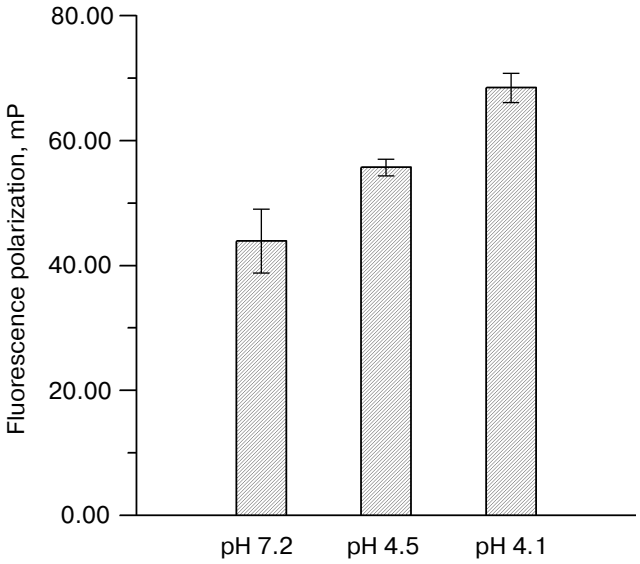

Fig. 5. Effect of pH on fluorescence polarization of C7-TCS. Ten minutes before the experiments, the sample was diluted with citrate-phosphate buffer at indicated pH value to 2 μM. Excitation wavelength was 280 nm for all pH values, and emission wavelength was fixed at the λ_{max} of Trp at the indicated pH. The values of I_{VV}, I_{VH}, I_{HV}, and I_{HH} were averages of three measurements at every pH value. The experiments were carried out at 25 ± 0.2°C.

Table 3. Fluorescence characteristics of C7-TCS at various pH values

Fluorescence parameters	pH values				
	7.2	4.5	4.1	3.64	2.98
λ_{max}, nm	337	335.5	334	333	332
Intensity	191.9	157.3	145.8	74.8	72.08

Note: Ten minutes before experiments the sample was diluted with citrate-phosphate buffer to 2 μM for C7-TCS and free Trp; final concentration of TCS was 1.5 μM. The fluorescence spectrum was scanned in the 295-400 nm interval with excitation at 280 nm.

Table 4. Percentages of various secondary structures in C7-TCS at different pH values

pH	Secondary structure, %				
	α-helix	β-sheet	β-turn	random coil	RMS
7.2	13.5	46.0	11.7	28.9	5.578
4.5	13.7	42.9	13.3	30.1	7.690
4.1	14.1	41.0	13.6	31.4	6.410

Note: Samples containing C7-TCS at a concentration of 3 μM were scanned at least four times at the rate of 100 nm/min and averaged. The pathlength of the quartz cell was 0.2 mm. The temperature of the sample compartment was maintained at 25 ± 0.2°C. The 200-250 nm spectrum was used for fitting. The fitting software used was J-700 for Windows Secondary Structure Estimate, version 1.10.00, provided by the JASCO Corporation, Hachioji City, Tokyo, Japan. RMS, root mean square.

DISCUSSION

Ribosome-inactivating proteins (RIP) are widely distributed in the plant kingdom and in certain bacteria. As the target substrate of RIP is ribosome in the cytosol, the translocation of internalized toxin into the cytosol is necessary to exert its RIP function. It is only recently that a breakthrough in the knowledge of the mechanism of such process for the type II RIPs was achieved.

In previous works [26-28] TCS, which is a type I RIP, was found to have pH-dependent membrane insertion ability. The membrane insertion of TCS could be induced at low pH values (e.g., at pH 4.6). In the present work the pH-dependent membrane insertion ability of C7-TCS was investigated using a monolayer system in

order to understand the relationship between this phenomenon and cytotoxicity of TCS.

The monolayer experiments have evidenced that the interaction between C7-TCS and lipid membrane is distinct from that of TCS in the following aspects. First, insertion of C7-TCS into DPPG monolayer is pH-dependent. However, it is continuously enhanced upon lowering sub-phase pH to 2.94, whereas TCS has pH_{max} at pH 4.6, which corresponds to pH in late endosome and lysosome. Second, the membrane insertion ability of C7-TCS into DPPG or DMPS monolayer is obviously lower than that of TCS. At pH 4.6, π_c for C7-TCS on a DPPG monolayer (or on a DMPS monolayer) is about 28 mN/m. Even maximum critical insertion pressure of C7-TCS at pH 2.94 is just 35 mN/m, which is still lower than that of TCS at pH 4.6 (38 mN/m). Third, usually membrane insertion of proteins proceeds in two major steps—docking to the membrane and inserting into it after a change in protein conformation. Various types of intermolecular interactions may be involved in the protein docking process, such as electrostatic and hydrophobic interaction, as well as specific interaction with the lipid head groups, etc. Through these interactions protein can be accumulated on the surface of the membrane and then insert into it. Previous works [36, 37] showed that for TCS electrostatic forces play an important role in the membrane docking, because the membrane insertion of TCS is affected by Na^+ in the sub-phase and lipid charge. However, for C7-TCS the electrostatic forces seem to be not necessary for membrane docking and insertion. In fact, an increase of Na^+ concentration in the sub-phase, even up to 400 mM, has no detectable effect on these processes. Then, C7-TCS interacts similarly with neutral and negatively charged lipid at pH 4.6, the critical insertion pressure on these lipid monolayers being very similar in both cases. Finally, C7-TCS can interact with the DPPG monolayer at neutral and even weakly alkaline pH, when it carries only a low positive charge, with π_c at pH 8.05 being approximately 27 mN/m. This value is similar to that for π_c at pH 4.6, which is about 28 mN/m (not shown here). These results suggest that another type of interaction facilitates membrane docking of C7-TCS instead of electrostatic interaction. Perhaps it is hydrophobic interaction. It is worth noting that there is no specific recognition between TCS and DPPG head groups [27].

The pH-dependent changes in the membrane insertion ability might reflect different conformational rearrangements of C7-TCS and TCS which they undergo upon interaction with the lipid monolayer. The fluorescence measurements support this supposition. It was found that pH value dramatically influences the fluorescence characteristics of C7-TCS. When pH was decreased from 7.2 to 2.98, the λ_{max} of Trp fluorescence showed a blue shift from 337 to 332 nm, and the fluorescence intensity of Trp was gradually lowered until pH reached 3.64. For comparison, the Trp fluorescence spectra of TCS were relatively invariant at all pH values, except that fluorescence intensity experienced slight variation, which might be caused by the pH-dependence of Trp quantum yield.

The λ_{max} blue shift of Trp suggests that this residue enters a hydrophobic microenvironment because of a conformational change in C7-TCS at low pH. The hydrophobic condition could be caused by exposing Trp to some hydrophobic regions of the C7-TCS molecule itself, by forming a new hydrophobic core through molecular aggregation, or both. The result of fluorescence polarization measurements suggested that low pH can induce oligomerization of C7-TCS molecules (similar to formation of diphtheria toxin aggregates at low pH). This effect was not found for TCS [36]. Therefore, it can be concluded that the decrease in pH could induce a significant conformational change in C7-TCS, which was not the case of TCS. Presumably, such conformational change occurred mainly at the level of tertiary structure, because the CD spectra of C7-TCS at different pH values were invariable.

The difference between C7-TCS and TCS in their pH-induced conformational response could be explained by the importance of Leu241 for the structure and function of TCS. The Leu241 is a conservative residue for many type I RIPs and the A-chain of type II RIPs, and plays a significant role in the hydrophobic interactions between the large and small domains of TCS. It contacts Trp192, Leu240, and Leu239 directly, thus forming a hydrophobic core of the smaller domain. In combination with hydrophobic residues from the larger domain, this hydrophobic core forms a hydrophobic region located on the side surface of the active center (Fig. 6). This hydrophobic region is important for keeping accurate folding of the active center. Therefore, deletion of Leu241 might exhibit the following effects on TCS: 1) the loss of hydrophobic core of the small domain resulting in a change in its conformation and exposure of Trp of the H7 helix to the medium; 2) weakening of hydrophobic interactions between the larger and smaller domains, resulting in reduced stability of the active center; and 3) disorganization of the TCS tertiary structure as a whole.

In conclusion, deletion of the last seven amino acid residues at the C-terminus dramatically affects the structure and function of TCS. The loss of Leu241 presumably results in weakened hydrophobic interactions that play a part in accurate folding of the active center. As a result, the tertiary structure of C7-TCS proves to be destabilized and its *in vitro* RIP activity decreases [23]. It should be pointed out that deletion of the C-terminal residues caused more significant reduction of C7-TCS cytotoxicity *in vivo* than its RIP activity *in vitro* [23]. This result might be explained by the distorted interaction between C7-TCS and lipid membrane. Conformational features of

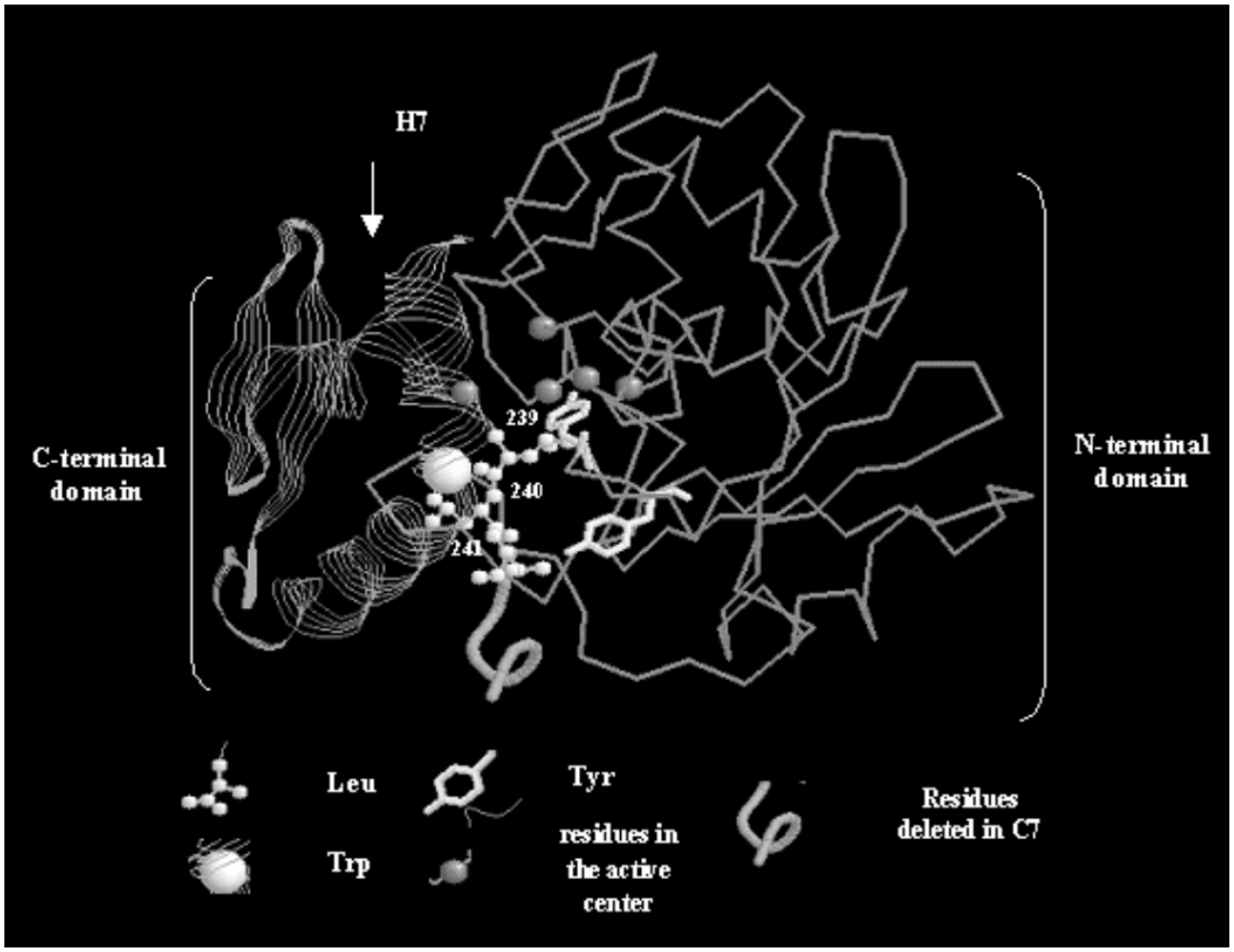

Fig. 6. Structural characteristics of trichosanthin. N-Terminal domain (residue 1 to 181, larger domain) is shown as backbone, and the C-terminal domain (residues 182 to 247, smaller domain) is shown as secondary structure. Residues deleted in C7-TCS (Leu241 to Ala247) are shown as cartoon form. Leu239, Leu240, and Leu241 are shown by ball and stick model. Trp192 at H7 is shown by a larger white ball and conserved five charged residues in the active center are shown by the smaller gray balls. Tyr70 and Tyr111 are shown as stick forms. It is noted that Leu241 contacts Trp192, Leu240, and Leu239 directly, thus forming a hydrophobic core of the smaller domain. In combination with hydrophobic residues from the larger domain, the hydrophobic core forms a hydrophobic region located on the side surface of the active center. Deletion of Leu241 to Ala247 might perturb the helical structure of H7 and weaken hydrophobic interaction between the smaller and larger domains of C7-TCS.

C7-TCS, making it different from TCS, results in the reduction of pH-dependent membrane insertion ability and pH-dependent formation of aggregates. As a consequence, at low pH (4.5-5.0) the amount of membrane inserted C7-TCS in the late endosome decreases. Perhaps, the internalized toxin remains in the lumen of the endosome, and undergoes degradation in the lysosome instead of further translocation into the cytosol, which predetermines reduced cytotoxicity of C7-TCS in K562 cells. By and large, the aforesaid supports the idea that pH-dependent membrane insertion of TCS is relevant to its translocation into the cytosol.

We would like to thank Dr. X. H. Han for his excellent technical assistance in fluorescence polarization experiments. This work was supported by the National Natural Science Foundation of China and Foundation of Ministry of Education, P. R. China.

REFERENCES

1. Yeung, H. W., Wong, D. M., Ng, T. B., and Li, W. W. (1986) *Int. J. Pept. Protein Res.*, **27**, 325-333.
2. Wang, Y., Qiang, R. Q., Gu, Z. W., Jin, S. W., Zhang, L. Q., Xia, Z. X., Tian, G. Y., and Ni, C. Z. (1986) *Pure. Appl. Chem.*, **58**, 789-798.
3. Zhang, J. S., and Liu, W. Y. (1992) *Nucleic Acids Res.*, **20**, 1271-1275.

4. Wu, S., Lu, X. H., Zhu, Y. R., Yang, J., and Dong, Y. C. (1998) *Sci. China Ser. C. Life. Sci.*, **41**, 174-180.
5. Endo, Y., Gluck, A., Chan, Y. L., Tsurugi, K., and Warl, I. G. (1990) *J. Biol. Chem.*, **265**, 2216-2222.
6. Law, L., Tam, P. P. L., and Yeung, H. W. (1983) *J. Reprod. Fert.*, **69**, 597-604.
7. Cheng, K. F. (1982) *Obstet. Gynecol.*, **59**, 494-498.
8. Chan, Y., Tong, M. K., and Lau, M. J. (1982) *Shanghai J. Chin. Med.*, **3**, 30-31 (in Chinese).
9. Pal, O. F., and Kirsten, S. (2000) *Curr. Opin. Cell. Biol.*, **12**, 407-413.
10. Blewitt, M. G., Chung, L. A., and London, E. (1985) *Biochemistry*, **24**, 5458-5464.
11. Montecucco, C., Schiavo, G., and Tomasi, M. (1985) *Biochem. J.*, **231**, 123-128.
12. Sandvig, K., and Olsnes, S. (1980) *J. Cell. Biol.*, **87**, 828-832.
13. Falnes, P. O., Ariansen, S., Sandvig, K., and Olsnes, S. (2000) *J. Biol. Chem.*, **275**, 4363-4368.
14. Papini, E., Sandona, D., Rappuoli, R., and Montecucco, C. (1988) *EMBO J.*, **7**, 3353-3359.
15. Sandvig, K., and van Deurs, B. (1996) *Physiol. Rev.*, **76**, 949-966.
16. Llorente, A., Rapak, A., Schmid, S. L., van Deurs, B., and Sandvig, K. (1998) *J. Cell Biol.*, **140**, 1-11.
17. Mukherjee, S., Ghosh, R. N., and Maxfield, F. R. (1997) *Physiol. Rev.*, **77**, 759-803.
18. Llorente, A., van Deurs, B., and Sandvig, K. (1998) *FEBS Lett.*, **431**, 200-204.
19. Mallard, F., Antony, C., Tenza, D., Salamero, J., Goud, B., and Johannes, L. (1998) *J. Cell Biol.*, **143**, 973-990.
20. Ghosh, R. N., Mallet, W. G., Soe, T. T., McGraw, T. E., and Maxfield, F. R. (1998) *J. Cell Biol.*, **142**, 923-936.
21. Suzuki, T., Yan, Q., and Lennardz, W. J. (1998) *J. Biol. Chem.*, **273**, 10083-10086.
22. Kirsten, S., and Bo, V. D. (1999) *FEBS Lett.*, **452**, 67-70.
23. Andrzej, R., Pal, O. F., and Sjur, O. (1997) *Proc. Natl. Acad. Sci. USA*, **94**, 3783-3788.
24. Philip, J. D., Susan, R. O., Jorgen, W., Sjur, O., Lynne, M. R., and Michael, L. (2001) *J. Biol. Chem.*, **276**, 7202-7208.
25. Luigi, B., Maria, G. B., and Fiorenzo, S. (1993) *Biochim. Biophys. Acta*, **1154**, 237-282.
26. Xia, X. F., and Sui, S. F. (1999) *Chin. Sci. Bull.*, **44**, 1892-1895.
27. Lu, Y. J., and Xia, X. F. (2001) *Biochim. Biophys. Acta*, 1-9.
28. Xia, X. F., and Sui, S. F. (2000) *Biochem. J.*, **349**, 835-841.
29. Chan, S. H., and Shaw, P. C. (2000) *Biochem. Biophys. Res. Commun.*, **270**, 279-285.
30. Shaw, P. C., Yung, M. H., Zhu, R. H., Ho, W. K. K., Ng, T. B., and Yeung, H. W. (1991) *Gene*, **97**, 267-272.
31. Zhu, R. H., Ng, T. B., Yeung, H. W., and Shaw, P. C. (1992) *Int. J. Peptide Protein Res.*, **39**, 77-81.
32. Wong, K. B., Ke, Y. B., Dong, Y. C., Li, X. B., Guo, Y. W., Yeung, H. W., and Shaw, P. C. (1994) *Eur. J. Biochem.*, **221**, 787-791.
33. Demel, R. A. (1974) *Meth. Enzymol.*, **32**, 539-545.
34. Han, X. H., Sui, S. F., and Yang, F. Y. (1996) *Thin Solid Films,* **284/285**, 789-792.
35. Wang, S. X., Cai, G. P., and Sui, S. F. (1998) *Biochem. J.*, **335**, 225-232.
36. Demel, R. A., London, Y., Geurts van Kessel, W. S. M., Vossenberg, F. G., van Deenen, L. L., et al. (1973) *Biochim. Biophys. Acta*, **311**, 507-519.
37. Perrin, F. (1926) *J. Phys. Radium*, **1**, 390-401.
38. Nasir, M. S., and Jolley, M. E. (1999) *Comb. Chem. High Throughput Screening*, **2**, 177-190.
39. Aucouturier, P., Preud'homme, J. L., and Lubochinsky, B. (1983) *Diagn. Immunol.*, **1**, 310-314.
40. Levine, L. M., Michener, M. L., Toth, M. V., and Holwerda, B. C. (1997) *Analyt. Biochem.*, **247**, 83-88.
41. Jameson, D. M., and Seifried, S. E. (1999) *Methods*, **19**, 222-233.
42. Lynch, B. A., Loiacono, K. A., Tiong, C. L., Adams, S. E., and MacNeil, I. A. (1997) *Analyt. Biochem.*, **247**, 77-82.
43. Chang, C. T., Wu, C. C., and Yang, J. T. (1978) *Analyt. Biochem.*, **91**, 13-31.